SITE EFFECTS IN EUROSEISTEST: A COMPARISON BETWEEN OBSERVATIONS AND MODELING

Francisco J CHÁVEZ-GARCÍA[1], Dimitris RAPTAKIS[2], Konstantia MAKRA[3] And Kyriazis PITILAKIS[4]

SUMMARY

This paper presents results of numerical modeling of site response for Euroseistest. Ground motion been simulated at the surface of this valley for vertically incident SH waves. The predominance of locally generated surface waves is clear in the synthetic seismograms. These results are then compared with an analysis of two events in the time domain. It is discussed in which sense it is possible to obtain a good fit between observations and 1D models, even though the real behavior involves locally generated Love waves. It is stressed that in order to predict ground motion in alluvial valleys the information contained in the phase cannot be neglected.

INTRODUCTION

The importance of local geology on destructive earthquake ground motion is largely recognized in Earthquake Engineering. However, there is not a widespread agreement as regards what could be the best way to estimate the amplification caused by site effects using observational data. One of the reasons for this is the very few site effect studies where both a detailed study of subsurface structure and numerous high quality observations of earthquake ground motion have been available. For this reason, several test sites were established in recent years (e.g., Turkey Flat, Ashigara valley). In Europe, in 1992, Euroseistest project was started with the aim of contributing high quality data to the site effect problem. General information and description of Euroseistest may be found in several publications (e.g., Pitilakis et al., 1995). Previous studies at Euroseistest have concerned the determination of the subsoil structure (Jongmans et al., 1998), evaluation of site effects from seismic records (Riepl et al., 1998) as well as numerical modelling of ground motion (Tolis et al., 1998). Recently, a reappraisal of the geophysical data gathered at this valley led to a revaluation of the geometry and mechanical properties of the valley (Raptakis et al., 1999). The result was an improvement on the previous benchmark model of the subsoil structure at Euroseistest. We take advantage of this model to take a fresh look at site effects at Euroseistest. We present a comparison between simulated and observed site effects in Euroseistest. Our purpose is to bring together observations and results of modeling and to improve our understanding of the physics of site effects at Euroseistest. A more detailed account of our results is given in Chávez-García et al. (1999).

NUMERICAL MODELING

Fig. 1 shows the model of the subsoil structure determined by Raptakis et al. (1999). This model that was elaborated after a careful reappraisal of all the data available. The description and properties of the sediments are given in Table 1. We have not introduced any simplifications in this structure, and have included in our model the irregular topography at the surface of the cross-section and anelastic attenuation, an important factor since the soft soils present in this valley cannot be considered as non-dissipative. The soil strata are cut by four faults.

We have used the 2D, SH-wave, finite difference method of (Moczo, 1989). This method allows modeling of a non-flat free-surface and the inclusion in the model the precise irregular shapes of the subsoil structure. The maximum accurate frequency for our computations of 4 Hz. The grid model was bounded with transparent boundaries. To verify that no unwanted artificial reflections were introduced by the finiteness of our grid, we computed results for two similar models, different only in the extension of the grid outside the valley The comparison showed clearly that no significant artificial reflections were generated at the transparent boundaries

[1]   *Instituto de Ingeniería, UNAM, Mexico*
[2]   *Lab. of Soil Mechanics and Foundations, Civil Eng. Dept., AU. Th., Greece*
[3]   *Lab. of Soil Mechanics and Foundations, Civil Eng. Dept., AU. Th., Greece*
[4]   *Lab. of Soil Mechanics and Foundations, Civil Eng. Dept., AU. Th., Greece*

of the model. Attenuation is taken into account through three relaxation mechanisms, at frequencies chosen to insure constant-Q in the frequency range of validity of the computations (from 0.1 to 4 Hz). The excitation to the model was given by vertical incidence of a plane SH wave, with a time variation in the form of a Gabor pulse.

The resulting time domain seismograms computed at the surface are shown in Fig. 2, low-pass filtered with a 3.5 Hz cutoff. The largest amplitudes are clearly dominated by locally generated Love waves. The asymmetrical structure of the valley generates strong Love waves at fault F4 with group velocity, U, about 210 m/sec and phase velocity, c, about 700 m/sec. Fault F1 generates similar Love waves, but with smaller amplitude. The Love waves generated by faults F1 and F4 are not affected by the presence of faults F2 and F3, indicating that they are guided by the topmost layers. Fault F3 generates an additional, faster Love wavetrain (U=300 m/sec, c=1250 m/sec), probably guided by the deeper layers, which have a significant discontinuity at this fault. A dispersion analysis of the 1D structure at the center of the valley (not shown) allows to identify these Love waves with the fundamental and first higher modes. The frequency content of each of those two modes of surface waves coincides with the minimum of the corresponding group velocity curves at about 0.8 and 2 Hz. We observe that topography around Profitis does not have a significant effect in the frequency band included in the synthetics.

We have computed transfer functions relative to input from the synthetics (Fig. 3). The center of the valley shows a peak of amplification at about 0.85 Hz. This peak is not homogeneous across the valley and breaks between 3000 and 4000 m distance. In Fig. 1 no significant geologic discontinuities are seen. Neither does Fig. 2 show any obvious amplitude change in this distance range. This is explained by Fig. 4, which shows the spectrogram of the synthetic at the position of TST. Fig. 4 shows that the energy that contributes to the "resonant" peak at 0.8 Hz is distributed all along the synthetic, including both 1D resonance and surface waves.

COMPARISON WITH OBSERVED SITE RESPONSE

Observation of site effects in Volvi basin has been an important objective of Euroseistest project. In 1994, a temporary recording campaign using 39 digital seismographs was carried out. The instruments were disposed in three networks: a line of 23 instruments crossing the valley between Profitis and Stivos; a line of 8 seismographs disposed parallel to the axis of the valley at its centre; and a small, cross-shaped array at the center of the valley of 8 instruments. The description of the experiment is presented in Riepl et al. (1998). In that study, analysis of the data was carried out in the frequency domain. It was observed that significant amplification was also present in the vertical component, with amplitude comparable to that observed for horizontal motion.

The analysis of Riepl et al. (1998) was thoroughly done in the frequency domain. As our synthetics stress the importance of surface waves in the site response, we decided to look into this dataset. However, we do not attempt to analyze the very large number of records obtained during the experiment. Rather, we have selected a well recorded event, the one that occurred on 06.25.94, had a local magnitude of 2.5 and was located 25 km to the SE of Euroseistest. It was recorded by 17 seismographs crossing the alluvial valley and by 7 stations of the dense array at the center of the valley. We rotated horizontal components in directions parallel and perpendicular to the valley's axis. First we examined the array crossing the valley. We filtered the records filtered in several frequency bands, trying to identify coherent wave pulses among the traces. Fig. 5 shows, for example, seismic section across the valley for the horizontal component of motion in the direction N59.5 E (SH motion). The traces have been low-pass filtered with a cutoff frequency of 3.5 Hz. We observe very large differences between the records along the section, however these differences concern more the duration than the amplitude of ground motion. We observe clear, large amplitude late arrivals at all stations in the distance range between 1.0 and 4.5 km. These late arrivals are very likely surface waves generated at the edges of the basin, however it was impossible to identify a single pulse arriving at different stations in any frequency band. This suggests that wavelengths are shorter than average spacing (about 400 m). The frequency of these late pulses lies below 2 Hz.

If the long duration of the records observed at the center of the valley is caused by short wavelength Love waves, then the dense array is appropriate to analyze these waves. However, the distribution of the 7 stations that recorded this event form an almost linear array due to malfunction of one station. In spite of this, we computed f-k spectra for different time windows and for a sequence of 0.4 Hz wide frequency bands between 0.3 and 3.0 Hz. Fig. 6 shows the results. Also in Fig. 6 are shown the dispersion curves expected for the fundamental and first higher mode of Love waves from the geotechnical profile at the center of the valley. In spite of aliasing problems we observe a good agreement between observed and theoretical dispersion curves. This analysis suggests that the S-wave window includes Love waves between 1 and 2 Hz, while the later coda of S-waves consists of Love waves between 1 and 3 Hz. The phase velocity is comprised between 300 and 400 m/sec, in good agreement with the results from modeling. Thus, wavelengths should be between 100 and 400, which explains why individual pulses could not be correlated among the stations of the larger array.

In addition to the seismograph networks, in Euroseistest operates a permanent accelerographic network. Previous studies of site effects using data from these instruments are those of Raptakis et al. (1998) and Dimitriu et al. (1998). In those studies, the emphasis was put on chracterising site response through its amplitude transfer function in the frequency domain. Dimitriu et al. (1998) concentrate on TST station, where they fit the empirical transfer functions with a computed transfer function for SH-wave incidence, using the incidence angle as a free parameter. It is remarkable the close fit obtained by Dimitriu et al. (1998) between observed and computed spectral amplitudes. This is in strong contrast with the results of our numerical simulations, where we observed the predominance of locally generated surface waves. For this reason we have chosen a single event recorded by the strong motion network, to check the role of surface waves in site response in this valley. We have chosen the event that occurred on 5.03.95, had a local magnitude of 5.3 and was located 32 km to the South-East of TST. The result was very similar to what we obtained from the weak motion records. The most striking differences between records outside the valley and those on the sediments were not in amplitude but in the duration of shaking. At stations within the valley, late arrivals with significant amplitude are readily identified.

We will now take a look at the borehole acceleration records for this earthquake, recorded at depths of 17 and 72 m, under TST surface station. We first aligned the arrival time of P wave in the vertical components, to insure an almost common time base for the three records, incurring in a very small error. Numerical modeling suggest that two modes of Love waves (fundamental and first higher mode) are important at 0.8 and at 2 Hz. For this reason we filtered the observed borehole records around these two frequencies. Fig. 7 shows, for example, the SH component of the three vertical records band-pass filtered between 0.4 and 1 Hz. The traces are very similar. The dashed, zero-phase lines in Fig. 7 follow peaks and troughs that are readily correlated among the traces. A very similar result (not shown) is obtained for the frequency band between 1.6 and 2.4 Hz. In Fig. 8 we have plotted the amplitudes of the peaks and troughs followed from trace to trace in the two frequency bands, 0.4 to 1.0 Hz and 1.6 to 2.4 Hz, as a function of depth, normalized by the value at the free surface. The thick lines in this figure show the theoretical modal shapes computed for the vertical profile at TST station. The symbols correspond to the amplitudes measured along the zero-phase lines of the three stations in the vertical array. The agreement between observed and predicted modal shapes is very good. Thus, the borehole records support our claim that, in the low frequency range, ground motion is dominated by locally generated surface waves.

CONCLUSIONS

We have taken advantage of a recent reinterpretation of field data that imprived the model of the subsoil structure at this valley. We have computed the response of this 2D structure to vertically incident SH waves. The results show that the dominant feature of site response are locally generated surface waves.

We have looked for evidence of these surface waves in earthquake data recorded at this site including both seismograph and accelerograph data. Our observations suggest that locally generated surface waves contribute significantly to ground motion, and that they appear at the same frequencies as resonance of vertically propagating shear waves. The velocity of these surface waves is consistent with modeling results and their wavelength should lie between 100 and 400 m. Thus, local heterogeneities will affect them significantly, which explains the difficulty of identifying common pulses common among the different stations.

We have shown that the fact that layering below TST is almost flat does not make this site a good candidate for 1D analysis. The dominant feature of site response at frequencies below 4 Hz are surface waves generated at the edges of the valley. Amplitude transfer functions give only partial information of site response. A good fit of this partial observation using 1D models cannot rule out the importance of 2D site effects. If 2D site effects are important, predictions of ground motion made on the basis of the 1D good fit will lead to large errors.

ACKNOWLEDGEMENTS

REFERENCES

Chávez-García, F.J., D. Raptakis, K. Makra, and K. Pitilakis (1999). Site effets at Euroseistest. Part 2. Results from 2D numerical modeling and comparison with observations, Soil Dyn. & Dyn. Struct., in press.

Dimitriu, P.P., C.A. Papaioannou, and N.P. Theodulidis (1998). EURO-SEISTEST strong-motion array near Thessaloniki, Northern Greece: a study of site effects, Bull. Seism. Soc. Am. 88, 862-873.

Jongmans, D., K. Pitilakis, D. Demanet, D. Raptakis, J. Riepl, C. Horrent, G. Tsokas, K. Lontzetidis, and P.-Y. Bard (1998). EURO-SEISTEST: determination of the geological structure of the Volvi basin and validation of the basin response, Bull. Seism. Soc. Am. 88, 473-487.

Moczo, P. (1989). Finite-difference technique for SH waves in 2-D media using irregular grids: application to the seismic response problem, Geophys. J. Int. 99, 321-329.

Pitilakis et al. (1995). EURO-SEISTEST. A European Test-Site for Engineering Seismology, Earthquake Engineering and Seismology, Final Scientific Report, task 4.3: Laboratory tests.

Raptakis, D., N. Theodulidis, and K. Pitilakis (1998). Data analysis of the Euroseistest strong motion array in Volvi (Greece): standard and horizontal-to-vertical spectral ratio techniques, Earthquake Spectra 14, 203-224.

Raptakis, D., F.J. Chávez-García, K. Makra, and K. Pitilakis (1999). Site effects at EUROSEISTEST: 2D model, observations and comparisons with 1D analysis, Soil Dyn. and Earthq. Engrg., in press.

Riepl, J., P.-Y. Bard, D. Hatzfeld, C, Papaioannou, and S. Nechstein (1998). Detailed evaluation of site response estimation methods across and along the sedimentary valley of Volvi (EURO-SEISTEST), Bull. Seism. Soc. Am. 88, 488-502.

Tolis, S., E. Faccioli and K. Pitilakis (1998). A 2D simulation of Euroseistest near Thessaloniki, Greece, in K. Irikura, K. Kudo, and H. Okada (eds.) The effects of surface geology on seismic motion 1, A.A. Balkema, 255-262.

Table 1

Layer	Decription	S-wave velocity	Density	QS
A	Silty-clayly sand	130	2.05	15
B	Silty sand and sandy clay	200	2.15	25
C	Marly silt and silty sand	300	2.08	30
D	Marly, sandy clay and clay silt	450	2.10	40
E	Alternating sublayers of clayly, silty sand and sandy clay with stones and gravels	650	2.16	60
F	Alternating sublayers of clayly, silty sand and sandy clay with stones and gravels	800	2.20	80
G*	Weathered schist bedrock	1,250	2.50	100
G	Gneiss basement	2,600	2.60	200
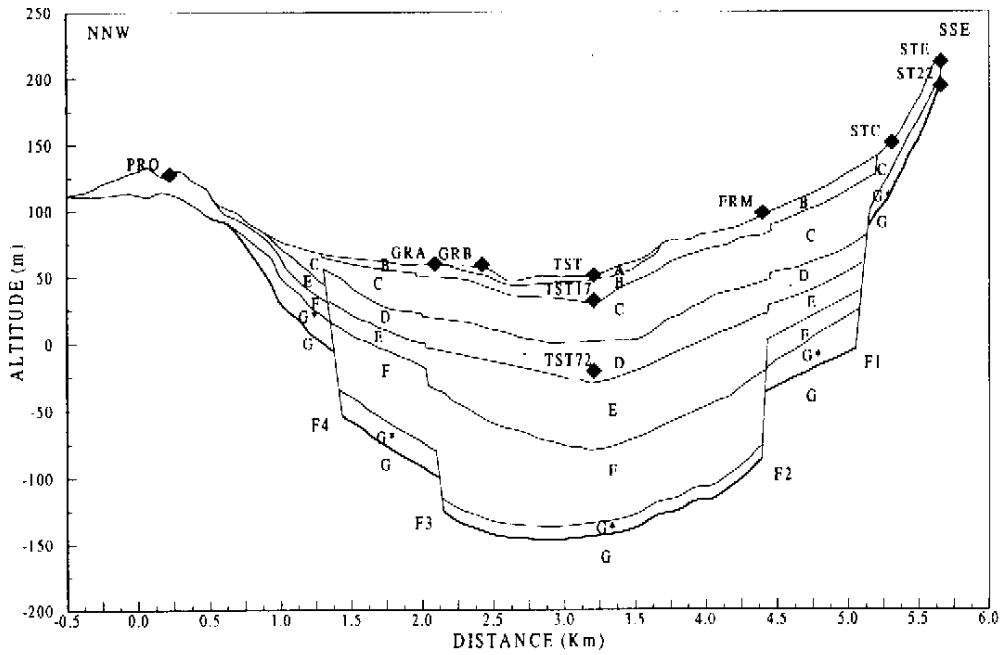
Figure 1. Final cross-section determined by Raptakis et al. (1999) for Volvi basin, between the villages of Profitis and Stivos. The solid diamonds show the location of the permanent strong motion network. Four faults (F1 to F4) and eight different strata (layers A to G) are identified. Properties of the material are given in Table 1. [After Raptakis et al., 1999.]
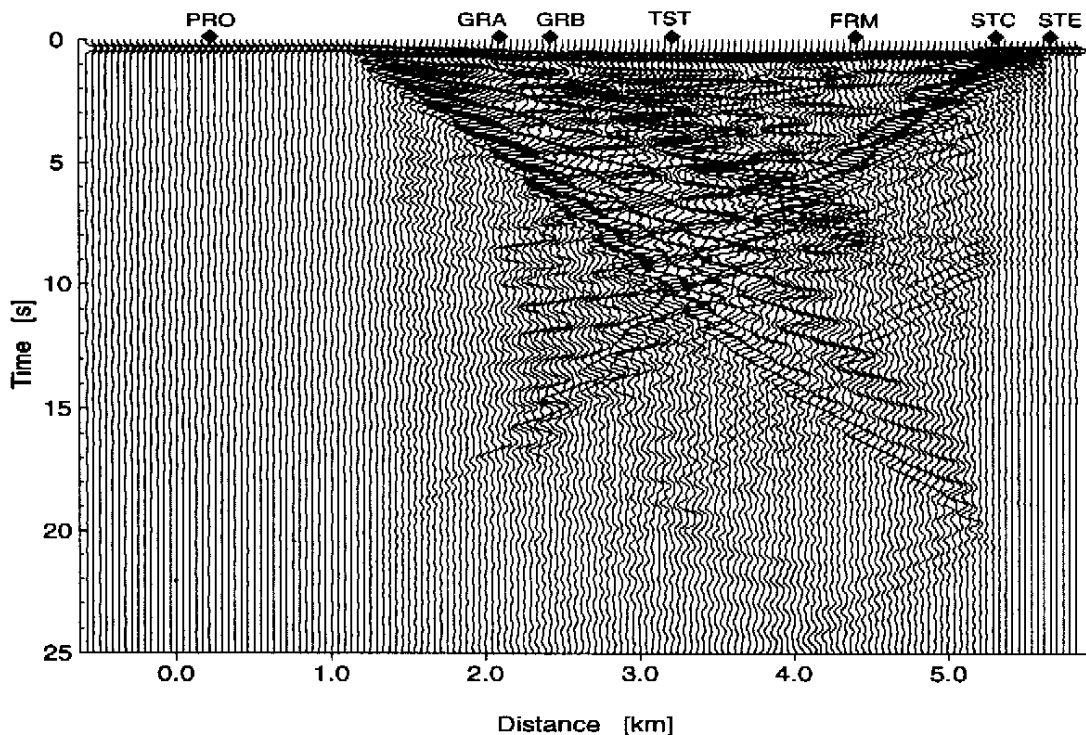
Figure 2. Seismic section computed at the surface of the 2D model shown in Figure 1 for vertical incidence of SH waves. The positions of the surface accelerographs of the permanent network have been indicated for reference. Traces have been low-pass filtered with a 3.5 Hz frequency cutoff. Anelastic attenuation was included in the computations.
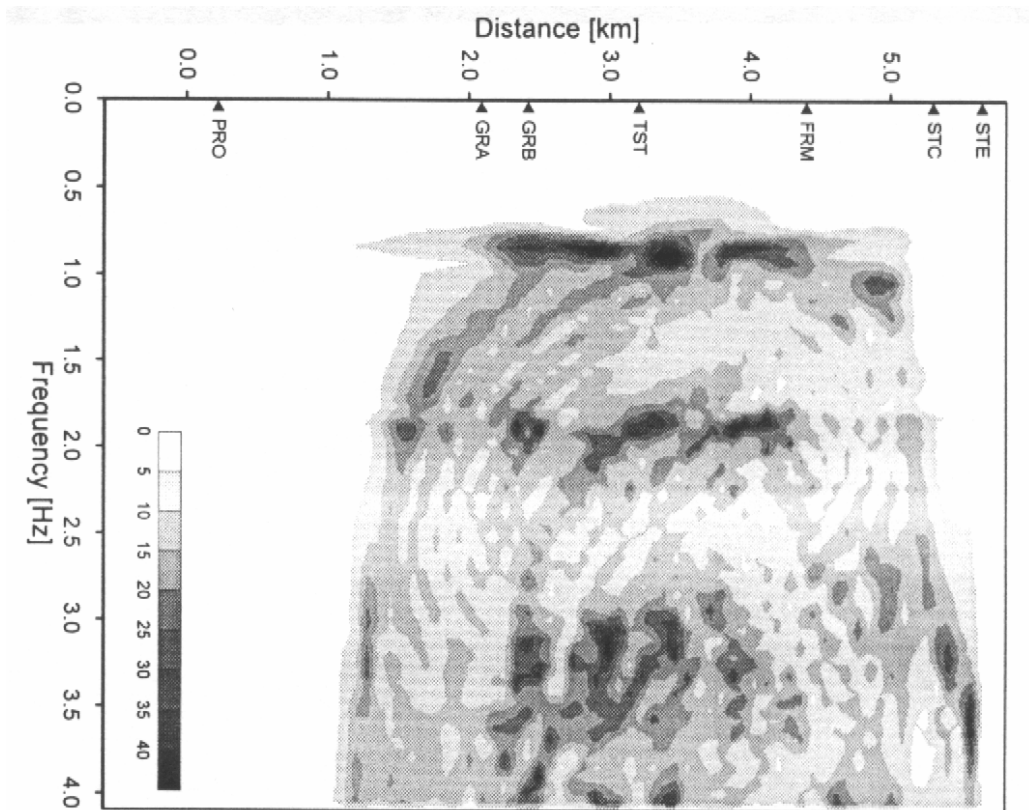
Figure 3. Theoretical transfer function for vertical incidence of SH waves on the model shown in Figure 1. This result was obtained from the synthetics shown in Figure 2. The positions of the surface accelerographs of the permanent network have been indicated for reference. We have not corrected for the free-field factor, thus the transfer function value in absence of the valley would be a factor of two.
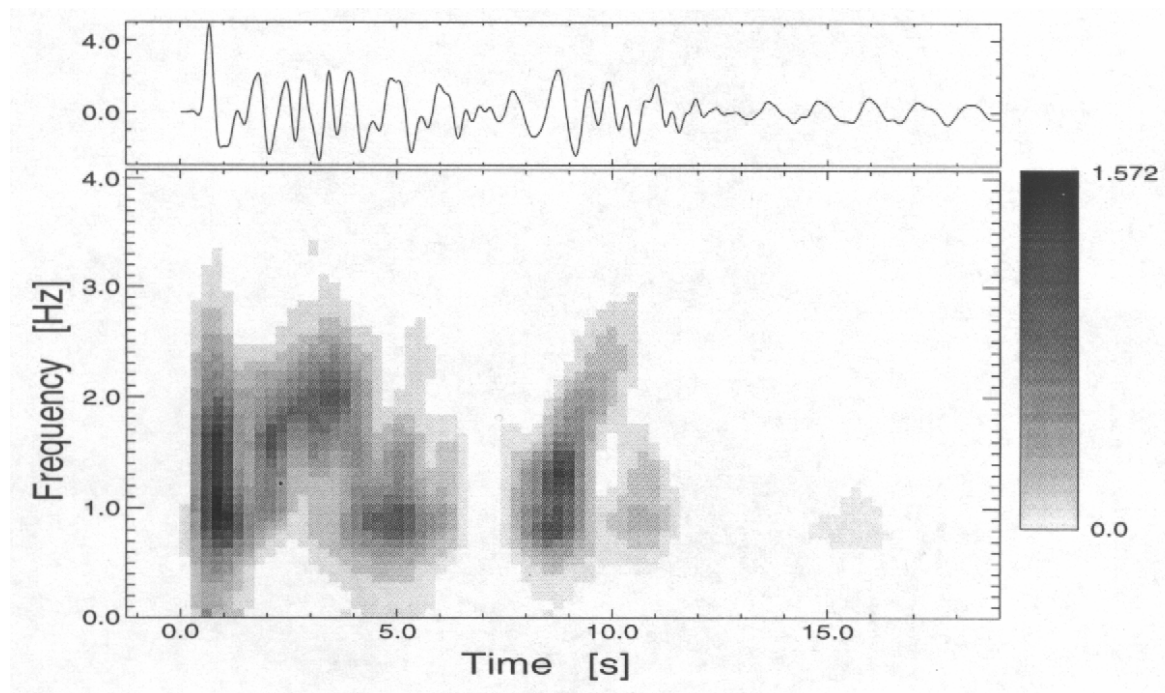
Figure 4. Evolutionary spectrum of the synthetic seismogram computed by finite differences for the location of TST in the 2D model of Figure 1. The corresponding trace is shown on top of the evolutionary spectrum. Before computing the spectrum, the trace was low-pass filtered with a 3.5 Hz frequency cutoff. Spectral amplitudes are given by the linear gray scale shown at the right of the figure.
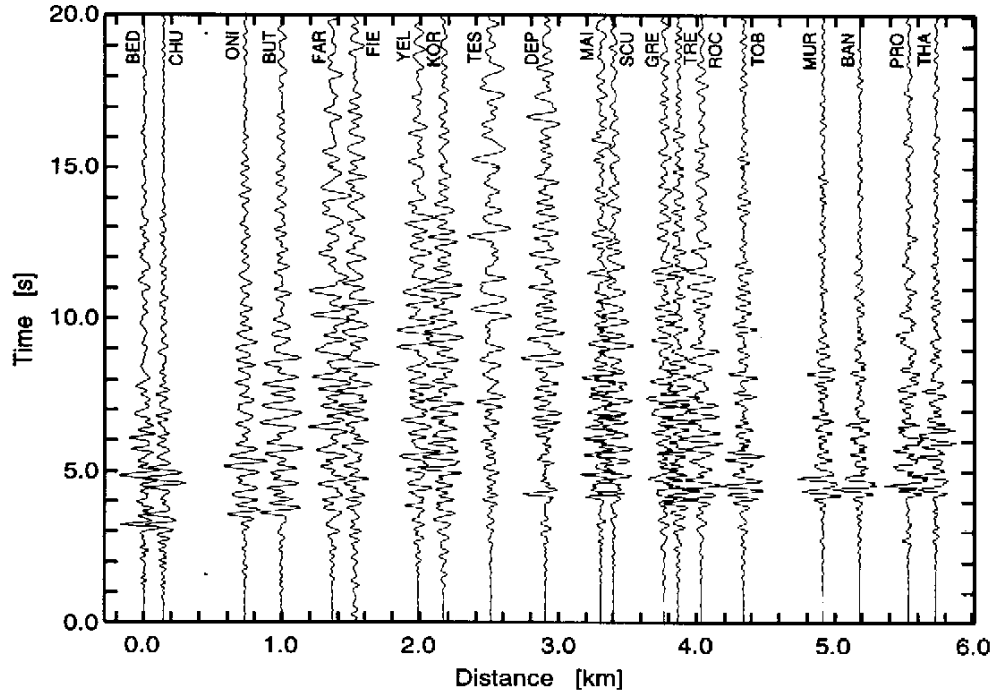
Figure 5. Seismic section obtained using the records of the Reftek array for the event of 06.25.94. The traces correspond to horizontal motion in the direction N59.5 E (SH motion). Distance is measured along the cross section of Figure 1 with an arbitrary origin. Traces have been low-pass filtered with a 3.5 Hz frequency cutoff. Amplitude scale is arbitrary but common to all the traces.
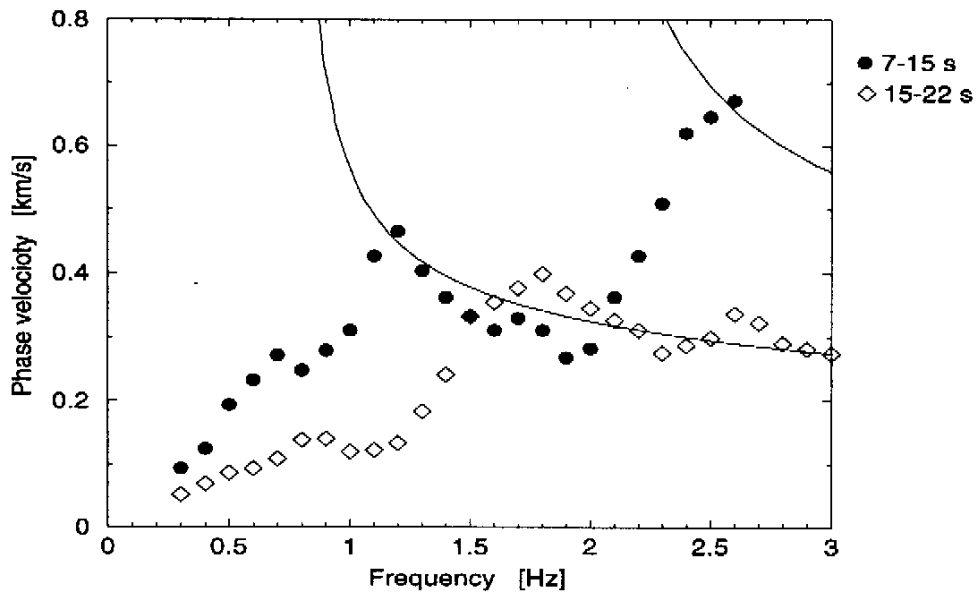
Figure 6. Results of f-k analysis for the event of 06.25.94 recorded by the dense array at the center of the valley. The results correspond to ground motion in the direction N59.5 E, i.e., SH motion. Each symbol corresponds to the maximum of a spectrum in the kx-ky diagram for a sequence of 0.4 Hz wide frequency bands between 0.3 and 3 Hz. Results are given for two different time windows corresponding to the S-wave (7 to 15 s) and the coda of S-waves (15 to 22 s), indicated with dotted lines in the upper panel. The solid lines correspond to the phase velocities computed for the vertical stratigraphy at the center of the valley.
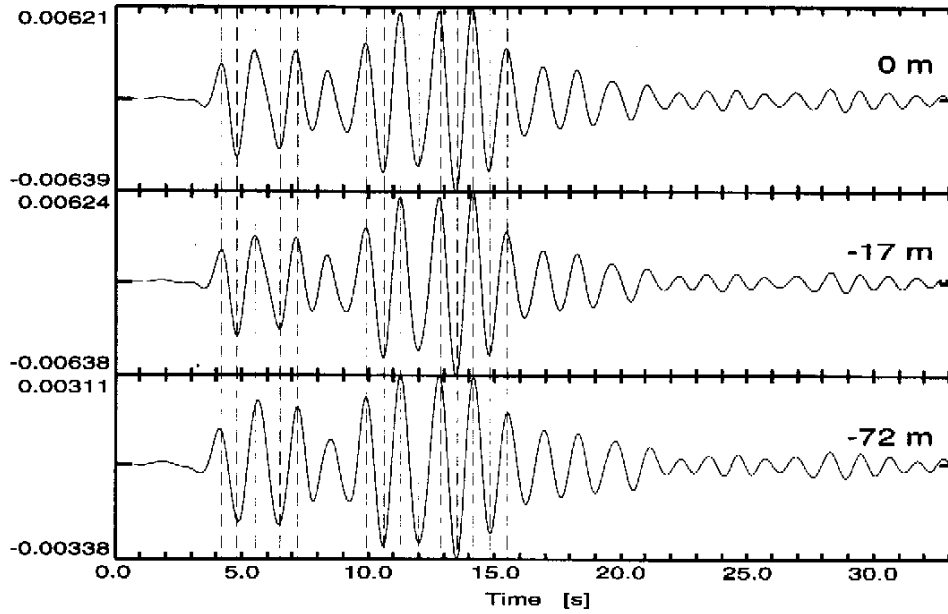
Figure 7. Transverse components of acceleration (in the direction N59.5 E, parallel to the valley's axis) recorded at the surface, and 17 and 72 m depth accelerographs at TST site for Arnea event. Traces have been band-pass filtered between 0.4 and 1 Hz. The dashed lines follow in-phase peaks and troughs for the three records. The amplitude scale for the traces is given in fractions of g.
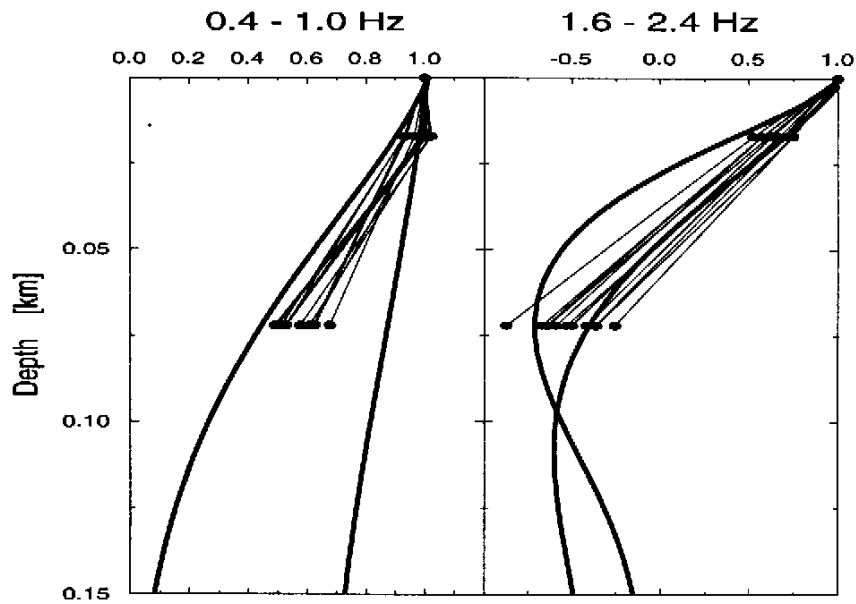
Figure 8. Observed an computed modal shapes at two frequency bands. Thick lines: computed modal shapes for the 1D profile at TST, fundamental mode in the left panel and first higher mode in the right panel. The two thick lines correspond to the limiting values of the frequency shown on top of each panel. Solid circles: amplitude of acceleration measured on the vertical accelerograph array in two frequency bands. Measured amplitudes have been normalized by the amplitude value at the surface.